IEEE Access
Multidisciplinary | Rapid Review | Open Access Journal

Received July 7, 2021, accepted July 16, 2021, date of publication July 26, 2021, date of current version August 3, 2021.

Digital Object Identifier 10.1109/ACCESS.2021.3099158

Real-Time Implementation of Adaptive Neuro Backstepping Controller for Maximum Power Point Tracking in Photo Voltaic Systems

ARUNPRASAD GOVINDHARAJ[1], (Student Member, IEEE), ANITHA MARIAPPAN[2], A. AMBIKAPATHY[1], (Member, IEEE), VIKAS SINGH BHADORIA[3], (Member, IEEE), AND HASSAN HAES ALHELOU[4], (Senior Member, IEEE)

[1]Galgotias College of Engineering and Technology, Greater Noida, Uttar Pradesh 201310, India
[2]Faculty of Engineering and Technology, Annamalai University, Chidambaram, Tamil Nadu 608002, India
[3]ABES Engineering College, Ghaziabad, Uttar Pradesh 201009, India
[4]Department of Electrical Power Engineering, Tishreen University, Latakia, Syria

Corresponding author: Hassan Haes Alhelou (alhelou@ieee.org)

ABSTRACT The efficiency of the low-cost renewable energy source i.e. solar is very poor due to inadequate extraction of maximum power. By employing the proper maximum power point tracking algorithm, the efficiency can be increased. An innovative adaptive backstepping neural network controller is proposed in this paper to extract the maximum power from the solar panels by tracking the desired photovoltaic array voltage in real-time. The maximum power is extracted indirectly by tuning the PV voltage to the desired PV voltage where the maximum power is attained at the desired PV voltage point. The desired photovoltaic array voltage is obtained from the linear regression method. The change in photovoltaic current caused by varying irradiance and temperature is approximated using the Chebyshev polynomials. The quicker steady-state and transient responses are accomplished and the computational burden of the photovoltaic system control law is reduced because of the orthogonal property of Chebyshev polynomials. The asymptotically stable system is obtained by tuning the weights of the neurons in accordance with the Lyapunov stability analysis. Also, Lyapunov control function of the backstepping control design procedure finds a control law by an innovative cubic equation interpretation, instead of resolving the first derivative of the control law, that diminishes the ripples in the duty cycle to make its appropriateness in real-time. A prototype is developed to validate the robustness of this controller in maximum power extraction at a faster time and the results confirm that adaptive backstepping neural network controller surpasses the performances of conventional backstepping controller and constant voltage PID controller.

INDEX TERMS Photo voltaic, Chebyshev neural network, MPPT, Lyapunov stability, Chebyshev polynomials.

I. INTRODUCTION

A huge increase in energy demand and fuel scarcity, the need of non-conventional energy sources has been enormously increasing [1]–[3]. The main form of air pollution is from power generation through conventional sources. Ultimately, the Photo Voltaic (PV) system is the most preferrable among the non-conventional energy sources since its minimum setting up budget. However, the solar panels exhibit low effectiveness in extracting maximum power since there is a lot of uncertainties in temperature, load resistance, irradiance and PV systems' nonlinear characteristics. Hence, power converters are chosen to achieve the maximum efficiency of PV systems for maximum power extraction [4], [5]. As the continuous current needs to be discharged in the PV systems to the load from the source, a boost converter is considered as an ideal choice for the proposed problem formulation. Because of the nonlinear behavior of PV cells to the change in temperature and irradiance, the necessary duty cycle has to be derived to extract maximum power. Hence, the scientists

The associate editor coordinating the review of this manuscript and approving it for publication was Lei Wu.

are doing broad research in the Maximum Power Point Tracking (MPPT) algorithms for PV systems to get the maximum power.

At first, researchers have developed two algorithms namely Incremental Conductance (IC) as well as Perturb and Observe (P&O). The P&O method perturbs the duty cycle and observes the power. The method iterates until the Maximum Power Point (MPP) [6]–[8]. But P&O hunts a new MPP for each time even after the maximum power, consequently, the solar panel voltage fluctuates resulting in larger oscillations. Moreover, for a particular change, it reacts slowly to perturb the duty cycle, henceforth it takes more time to accomplish the stable maximum power. On the contrary, IC reduces the oscillations completely and the individual control circuitry is needed to carry out the algorithm and it takes more time to attain the stable maximum power [9], [10]. The aging effect and partial shading of the PV panels make them less efficient in extracting the maximum power, therefore, the maximum power must be optimized globally. But P&O and IC try to optimize the maximum power locally which generates low power.

Ripple correlation control techniques [11], [12] for tracking the MPP reduces ripples in comparison with hill climbing techniques. However, it prolongs the time in extracting the generated MPP. In low radiances, the MPP cannot be extracted for the generated power. Fuzzy logic methods [13] do not require any mathematical model. But they require the system input and output information that depends on human knowledge. MPP tracking in PV array rests on fuzzy logic rules. Conversely, the MPP cannot be tracked when the system information is less. Similarly, artificial intelligence [14] methods train the input and output data of the solar panel that helps in obtaining the desired MPP. From the generated power, desired MPP extraction is not possible with large variation in input and output of the controller from the trained data due to uncertainties in the PV array.

The Fuzzy Logic Controller (FLC) [15], [16] shows enhanced steady-state and transient responses in comparison with the above methods which consist of fuzzifier and defuzzifier. The FLC is designed based on the rules. Hence, it becomes more difficult for the computation of rules to the FLC, and for the broad range of disturbances, the maximum power cannot be attained successfully. As in the case of partial shading condition, instead of optimizing globally, it tries to optimize locally which reduces the efficiency of the controller.

In the linear Proportional Integral Derivative (PID) controller [17], [18], by making power as the desired value, the maximum power cannot be endured as it results in larger oscillations. Hence, the researchers had gone for constant voltage PID [19] and constant current PID [20] control approaches. The operating range of PID controllers is obtained by the gain parameters and it cannot function beyond the specified range which results in instability of the PV system. Henceforth, the linear controllers are unable to use for the extensive functional range. Hence, the nonlinear techniques are most suited.

The majority of the nonlinear techniques work under rigorous boundaries [21], [22]. One such technique is the sliding mode controller. Sliding Mode Control (SMC) [23], [24] is a robust and effective tool in designing control structure for nonlinear models having external influences and uncertainties. It is used where the implementation requires robustness and is of highest priority. Sliding mode control is based on variable structure systems made with independent structures having various properties and a switching logic between them. At the point when the system moves on sliding surface, it is said the system slides. At that point a sliding mode happens near a switching surface when the system state vector is directed to do it. By definition, a surface $S(x) = 0$ is attractive when either trajectories beginning in the surface stay in it, or trajectories beginning externally to the surface tend to it. Therefore, it can be able to obtain the closed-loop response which ensures asymptotic stability and yet there is no assurance that this will occur in limited time particularly under uncertainty. However, for the broad range of disturbances caused by the system, the robustness of the controller is not guaranteed.

Feedback linearization method [25] changes a nonlinear system to a linear system by disposing of the imminent nonlinear characteristics of the system. Albeit this technique has palatable execution, one of the significant downsides is that it requires precise parameters of the system to accomplish the ideal control target and operations. In fact, exact parameters of a solar PV systems cannot be determined precisely.

In [26] authors had discussed about the extraction of maximum power using augmented state feedback linearization method in which the nonlinear system is linearized using the transformational matrix that is obtained by the non-linear control theory. In the augmented state feedback linearization method, the control law is tuned to get the desired power which is obtained using the ANN. As the control law is tuned to get the desired power which will results in more fluctuations and takes more time to attain its desired value.

Model Predictive Controller [27] operates under constant switching frequency making the design of filter easier. This controller provides several other benefits such as fast dynamic response, accurate reference tracking, and constant switching frequency. But this method also faces same drawback as the one mentioned above i.e., it requires the exact parametric information of the system.

To alleviate this, Backstepping Controller (BSC) had been introduced [28], [29]. Backstepping design can be applied to a class of non-linear systems as long as the internal dynamics are stabilized. Considering a second-order non-linear system of the form

$$\dot{x}_1 = f_1(x_1) + g_1(x_1)\, x_2$$
$$\dot{x}_2 = f_2(x_1, x_2) + u$$

First select a desirable value of x_2 possibly a function of x_1, denoted by x_{2d}, such that in the ideal system

$\dot{x}_1 = F_1(x_1, x_{2d})\, x_1(t)$ tracks steadily towards the desired x_{1d}. Then in a second step, select x_3 to be x_{3d}, so that x_2 tracks x_{2d} and this process is repeated. Finally, select u(t) such that x_m tracks x_{md}. The control law is obtained based on the Lyapunov stability function which ensures an asymptotically stable system. But for the backstepping control, the exact understanding of disturbances is needed. This drawback has been overcome by the adaptive backstepping control approach where the uncertainties are modeled by adaptive means of estimation [30]–[32]. Many robust and adaptive procedures exist which implement the above backstepping method. In adaptive backstepping control approach, the uncertainties are approximated to the approximation function [33]. Thus, the disturbances produced by the broad range of variation in the irradiance and temperature can be eliminated. The main drawback of this technique is that it will take more time to analyze exact uncertainties caused by variation in the irradiance and temperature, which greatly influences the static and dynamic characteristics of the PV system.

The disturbances can be approximated by the estimated function to understand the properties of the uncertainty. The approximation function is obtained based on the intelligent controllers such as fuzzy logic and neural network [34], [35] in which the uncertainty caused by both internal and external disturbances are approximated to either neural network or fuzzy logic without changing the mathematical model. Out of these, fuzzy logic needs rules for the estimation of disturbances caused by the system [36]–[39]. The complex rules of fuzzy logic create problems while updating the weight update law.

In the neural network, the weights are updated online based on the uncertainty caused by the disturbances which do not require initial training that result in the minimum computational problem. The Radial Basis Function (RBF) [40], [41] polynomial is not preferred because every node in the hidden layer has to compute the RBF function based on the different center values which result in the computation being more intense. Also, it does not have orthogonal property. The two known orthogonal polynomials are Chebyshev polynomials [42] and Legendre polynomials [43]. The Chebyshev polynomial is preferred as it gives the best approximation solution with minimum error property and different norms. It also requires fewer neurons as compared with RBF because it evaluates the power series.

This research is inspired by the aforementioned transient and steady state issues caused by the uncertainties and looks for an efficient way to approximate the uncertainties caused in obtaining the maximum power with enhanced steady state and transient responses, improving whole system efficiency, ensuring the robustness of the system and simultaneously improved dynamic performances with least error indices.

Adaptive Backstepping Controller Chebyshev Neural Network Controller (ABCNNC) is proposed in this paper, to extract the maximum power from solar panels based on the desired PV array voltage obtained by the linear regression method using the MPPT algorithm. In the MPPT algorithm, the disturbances caused by the change in PV current are estimated using the Chebyshev polynomials by which the maximum power is extracted with enhanced steady-state and transient responses.

The foremost goals of this work are:

1) To evaluate the disturbances instigated by the PV current due to change in irradiance and temperature and to get an asymptotically stable system through online tuning of weights of the neurons in regard to the Lyapunov stability analysis.

2) The necessary control law to obtain the desired PV array voltage obtained by the linear regression method is found by an innovative way of resolving the cubic equation instead of evaluating for the derivative of the control law from the Lyapunov Control Function.

3) To design a prototype in the laboratory to confirm its suitability in real-time.

4) To get enhanced steady-state and transient responses by the estimation of the disturbances produced by the PV systems.

This paper is structured as follows. The modeling of PV array, solar panel reference voltage generation, and problem statement is given in section 2. Section 3 defines the design of the ABCNNC. Section 4 shows the stability analysis for the PV system. Section 5 depicts the assessment of the steady-state and transient performance of the ABCNNC in simulation. Experimental results and discussion are portrayed in Section 6. Section 7 comprises the conclusion and future work.

II. SYSTEM MODELLING AND PROBLEM STATEMENT

A single diode PV module along with a boost converter that is used to extract maximum power from the solar panel is depicted in figure 1. The solar panel module has a current source I_{pv}, that gives the input power dependent on the irradiance and temperature of the environment, parasitic resistance R_p which arise because of the leakage current of the p-n junction within the PV cell, series resistance R_s which is caused by the metal contact used for connecting the PV cells, and internal diode D_1. The boost converter module has an input capacitance C_i, bulk inductor L, MOSFET switch SW, diode D_2, and load resistor R. The MOSFET is controlled by the pulses generated by Pulse Width Modulation (PWM) technique to extract maximum power from the PV panel. In the PWM technique, the pulses are generated for the

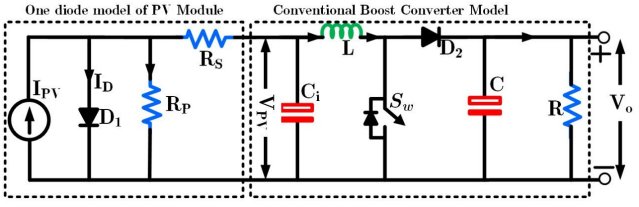

FIGURE 1. Boost converter based one diode model solar panel module.

control input u which is the fraction of ON time, to the total period of the pulses generated by the processor. The converter works in Continuous Conduction Mode (CCM), in which during the ON time of the pulses, the inductor will get charged linearly and the charge stored in the capacitor C will get discharged to load resistor as the MOSFET is in ON state and diode D_2 is in OFF state. During the OFF time, the power in the inductor along with power generated from the solar panel gives the output to the load resistor and the capacitor C is charged. Hence the average output voltage of the load resistor is boosted as compared with the solar panel output voltage.

Let x_1, x_2, and x_3 be the solar panel voltage (V_i), boost converter inductor current (I_L), and load voltage (V_O) respectively. Then the state-space modeling for the solar panel is given by

$$\dot{x}_1 = \frac{I_{pv}}{C_i} - \frac{x_2}{C_i} \tag{1}$$

$$\dot{x}_2 = -(1-u)\frac{x_3}{L} + \frac{x_1}{L} \tag{2}$$

$$\dot{x}_3 = (1-u)\frac{x_2}{C} - \frac{x_3}{RC} \tag{3}$$

Due to variations in temperature and irradiance, the solar cell current is more sensitive. Hence this causes unwanted changes in the transient and steady-state responses which deprive the net efficiency of the system.

A. SOLAR PANEL REFERENCE OUTPUT VOLTAGE GENERATION

To design the controller of any closed-loop system, the reference value should need to be known to tune it to the desired value. Hence in this manuscript, for all three controllers, the PV output voltage is tuned based on the reference PV output voltage. The reference PV voltage is obtained with respect to the irradiance and temperature of the solar cells. To get the desired PV voltage, the PV characteristic curve is obtained using simulation parameters shown in table 1 for different irradiance and temperature. For each temperature and irradiance variation, the MPP varies. In MATLAB, various MPP and corresponding PV voltage from the PV curve are noted by keeping Temperature (T) at 25°C and by changing the Irradiance (I) from 1400 W / m^2 to 600 W / m^2 as in figure 2. Similarly, various MPP and the corresponding PV voltage from the PV curve are noted by keeping I as 1000 W / m^2 and by varying T from 45°C to 10°C as depicted in figure 3. By the multiple linear regression method, the equation for reference PV voltage (V_{pvr}) and reference maximum power (P_{maxr}) are obtained and are given by

$$V_{pvr} = 34.72 - (0.00109^*I) - (0.12502^*T) \tag{4}$$

$$P_{maxr} = 41.3125 + (0.243^*I) - (1.055^*T) \tag{5}$$

TABLE 1. Solar panel parameters.

Solar Panel Parameters	Value
Temperature (T)	25°C
Irradiance level (I)	1000 W/m^2
Solar cells in parallel (N_p)	1
Solar cells in series (N_s)	1
Cells per module	60
Solar cell open circuit voltage (V_{oc})	38 V
Solar cell short circuit current (I_{sc})	8.80 A
Voltage at maximum power (V_{mp})	30.50 V
Current at maximum power (I_{mp})	8.56 A
Series resistance (R_s)	0.36302 Ω
Shunt resistance (R_p)	2800.4336 Ω

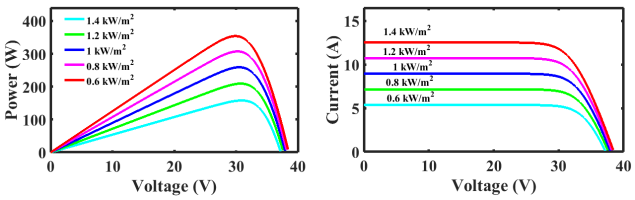

FIGURE 2. PV array curves at constant temperature with varying irradiance.

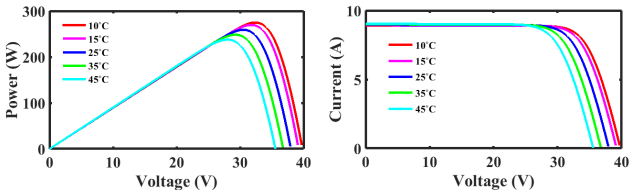

FIGURE 3. PV array curves at constant irradiance with varying temperature.

III. PROPOSED ABCNNC FOR THE PV SYSTEMS

The proposed controller is designed to get the maximum power from the PV panels by tuning it to the desired PV reference voltage which is obtained by the multiple linear regression method. The tuning of the PV voltage is done by changing the control law to find the desired PV array voltage. The control law of the ABCNNC is found based on the weights of the Chebyshev Neural Network (CNN) which is being updated based on the online weight update law that depends on the error value of PV output voltage as depicted in figure 4.

The main objective of the ABCNNC is to obtain the duty cycle which makes the error variable $Z_1 = x_1 - V_{pvr}$ to zero by enforcing the error variables $Z_2 = x_2 - x_{2d}$ and $Z_3 = x_3 - x_{3d}$ to zero. The online weight update law to estimate the weights for any change in irradiance and temperature of the CNN is updated using the error variable Z_1. The updated weight value is fed to CNN which quickly estimates the value of solar current for any change in irradiance and temperature which updates the control law fed to PWM. The duty cycle is calculated by solving the cubic equation which is obtained from the Lyapunov control function.

A. APPROXIMATING THE SOLAR CURRENT TO CNN

Because of its orthogonal property which does not make the system unstable in any condition and its ability to converge

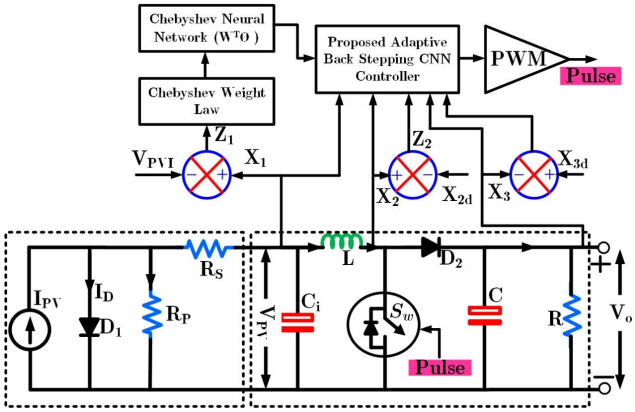

FIGURE 4. Proposed controller for the PV systems.

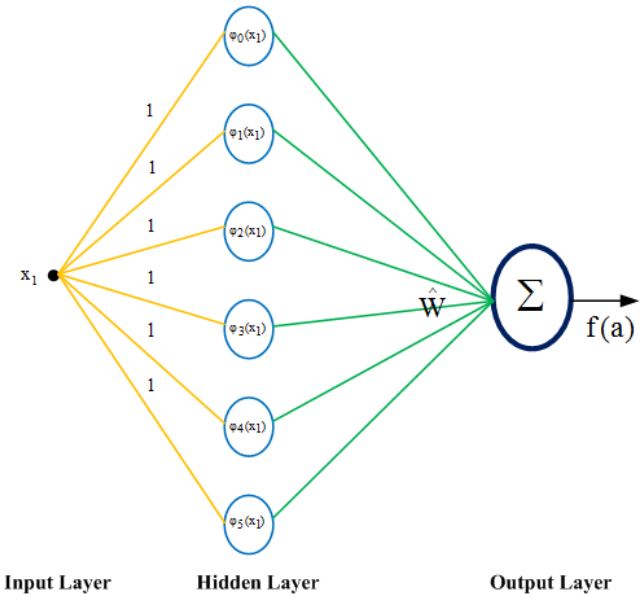

FIGURE 5. Chebyshev neural network structure for the proposed controller.

high power series, CNN is preferred for the estimation of uncertainties in the proposed algorithm and the structure of the neural network is given in figure 5.

The Chebyshev polynomials (φ) is updated using the recursive formula

$$\varphi_{p+1}(a) = 2a\varphi_p(a) - \varphi_{p-1}$$

where $\varphi_0(a) = 1$, $\varphi_1(a) = a$ and p represents p_{th} neuron value

$$\left(\varphi_p(a), \varphi_q(a)\right) = \int_{-1}^{1} \frac{\varphi_p(a), \varphi_q(a)}{\sqrt{(1-a^2)}} da$$

$$\left(\varphi_p(a), \varphi_q(a)\right) = \begin{cases} 0 & p \neq q \\ \pi & p = q = 0 \\ \frac{\pi}{2} & p = q \end{cases}$$

The approximation function is defined as

$$f(a) = W^T\varphi = \sum_{p=0}^{m} w_p\varphi_p$$

where $W^T = [w_1, w_2 \ldots\ldots w_m]$ are the weights of the neural network, $\varphi = [\varphi_1, \varphi_2 \ldots\ldots .\varphi_m]$ are the Chebyshev polynomial and m = total number of neurons.

In the proposed controller from equation (1), the unknown solar current (I_{pv}) which varies due to the change in the irradiance and temperature is approximated using the approximation function f (a). Then equation (1) becomes

$$\dot{x}_1 = \frac{W\varphi}{C_i} - \frac{x_2}{C_i} \tag{6}$$

B. STEP 2: DETERMINING THE LYAPUNOV CONTROL FUNCTION

The varying error value Z_1 is defined as

$$Z_1 = x_1 - V_{pvr} \tag{7}$$

Differentiating the above equation

$$\dot{Z}_1 = \dot{x}_1 - \dot{V}_{pvr} \tag{8}$$

By Substituting (6) in (8)

$$\dot{Z}_1 = \frac{W\varphi}{C_i} - \frac{x_2}{C_i} - \dot{V}_{pvr} \tag{9}$$

To minimize the error Z_1, a new virtual control input (x_{2d}) is derived which acts as a reference value for the second state variable. This will enforce the error Z_1 to zero by enforcing $x_2 = x_{2d}$.

Put $\dot{Z}_1 = -c_1Z_1$ in (9) where c_1 is the gain constant and solve for x_{2d}

$$x_{2d} = \hat{W}\varphi + C_ic_1Z_1 - C_i\dot{V}_{pvr} \tag{10}$$

The new error variable Z_2

$$Z_2 = x_2 - x_{2d} \tag{11}$$

Equation (11) can be rewritten as

$$x_2 = Z_2 + x_{2d} \tag{12}$$

By Substituting (12) in (9) $\dot{Z}_1$ can be rewritten as

$$\dot{Z}_1 = \frac{W^T\varphi}{C_i} - \frac{(Z_2 + x_{2d})}{C_i} - \dot{V}_{pvr} \tag{13}$$

Incorporating x_{2d} in equation (10) to the above equation and by solving $\dot{Z}_1$ becomes

$$\dot{Z}_1 = \frac{W^T\varphi}{C_i} - \frac{\hat{W}^T\varphi}{C_i} - \frac{Z_2}{C_i} - c_1Z_1 \tag{14}$$

$$\hat{W} = W - \tilde{W} \tag{15}$$

where $\hat{W}$ is the estimation of weight value and $\tilde{W}$ is the estimated error of the weight value.

By Substituting (15) in (14)

$$\dot{Z}_1 = \frac{\tilde{W}^T \varphi}{C_i} - \frac{Z_2}{C_i} - c_1 Z_1 \tag{16}$$

Taking time derivative of equation (10) and by substituting (8) $\dot{x}_{2d}$ can be written as

$$\dot{x}_{2d} = \dot{\hat{W}}^T \varphi + C_i c_1 \left(\dot{x}_1 - \dot{V}_{pvr}\right) - C_i \ddot{V}_{pvr} \tag{17}$$

By Substituting (6) in (17) and by solving the above equation

$$\dot{x}_{2d} = \left(-c_1 x_2 + c_1 W^T \varphi + \dot{\hat{W}}^T \varphi - C_i c_1 \dot{V}_{pvr} - C_i \ddot{V}_{pvr}\right) \tag{18}$$

Differentiating the equation (11)

$$\dot{Z}_2 = \dot{x}_2 - \dot{x}_{2d} \tag{19}$$

By incorporating equation (2) in (19), $\dot{Z}_2$ can be rewritten as

$$\dot{Z}_2 = -(1-u)\frac{x_3}{L} + \frac{x_1}{L} - \dot{x}_{2d} \tag{20}$$

To minimize the error Z_1 and Z_2, a new virtual control input (x_{3d}) is derived which acts as a reference value for the third state variable which will enforce the error Z_1 and Z_2 to zero by imposing $x_3 = x_{3d}$.

Put $\dot{Z}_2 = \frac{Z_1}{C_i} - c_2 Z_2$ is the gain constant and solve for x_{3d}

$$x_{3d} = \frac{L}{(1-u)}\left(-\frac{Z_1}{c_i} + c_2 Z_2 + \frac{x_1}{L} - \dot{x}_{2d}\right) \tag{21}$$

The new error variable Z_3 is

$$Z_3 = x_3 - x_{3d} \tag{22}$$

The above equation can be rewritten as

$$x_3 = Z_3 + x_{3d} \tag{23}$$

By substituting (23) in (20) $\dot{Z}_2$ can be written as

$$\dot{Z}_2 = -(1-u)\frac{(Z_3 + x_{3d})}{L} + \frac{x_1}{L} - \dot{x}_{2d} \tag{24}$$

By substituting (21) in (24)

$$\dot{Z}_2 = -(1-u)\frac{Z_3}{L} + \frac{Z_1}{C_i} - c_2 Z_2 \tag{25}$$

By substituting (18), (11) and (7) in (21)

$$x_{3d} = \frac{L}{(1-u)} \times \begin{pmatrix} -\frac{(x_1 - V_{pvr})}{C_i} + c_2(x_2 - x_{2d}) + \frac{x_1}{L} + c_1 x_2 \\ -c_1 W^T \varphi - \dot{\hat{W}}^T \varphi + C_i c_1 \dot{V}_{pvr} + C_i \ddot{V}_{pvr} \end{pmatrix} \tag{26}$$

By incorporating (10) in (26) x_{3d} can be rewritten as

$$x_{3d} = \frac{L}{(1-u)} S_2 \tag{27}$$

where, S_2 as shown at the bottom of the page.

By differentiating (27)

$$\dot{x}_{3d} = \frac{L}{(1-u)}\left(S_1 + \frac{\dot{u}}{(1-u)}\left(x_{3d}\,(1-u)\right)\right) \tag{28}$$

where, S_1 as shown at the bottom of the page.

By Substituting (27) in (28) $\dot{x}_{3d}$ can be rewritten as

$$\dot{x}_{3d} = \frac{L}{(1-u)^2}\left((1-u)\,S_1 + \dot{u}\,(L S_2)\right) \tag{29}$$

Taking time derivative of (23)

$$\dot{Z}_3 = \dot{x}_3 - \dot{x}_{3d} \tag{30}$$

Substituting (4) in (30)

$$\dot{Z}_3 = (1-u)\frac{x_2}{C} - \frac{x_3}{RC} - \dot{x}_{3d} \tag{31}$$

The Lyapunov function candidate is selected such that the error value Z_1, Z_2, and Z_3 should disappear while obtaining the asymptotic stable system. For the proposed controller the Lyapunov function candidate is

$$V = \frac{1}{2}Z_1^2 + \frac{1}{2}Z_2^2 + \frac{1}{2}Z_3^2 + \frac{1}{2}\tilde{W}^T P^{-1} \tilde{W} \tag{32}$$

where P is the adaptation rate.

$$S_2 = \begin{pmatrix} x_1\left(\frac{-1}{C_i} - C_i c_1 c_2 + \frac{1}{L}\right) + x_2\,(c_1 + c_2) - \hat{W}^T \varphi\,(c_1 + c_2) \\ -\dot{\hat{W}}^T \varphi + V_{pvr}\left(\frac{1}{C_i} + C_i c_1 c_2\right) + \dot{V}_{pvr}\,(C_i c_1 + C_i c_2) + C_i \ddot{V}_{pvr} \end{pmatrix}$$

$$S_1 = \begin{pmatrix} x_1\left(\frac{c_1 + c_2}{L}\right) + x_2\left(\frac{1}{C_i^2} + c_1 c_2 - \frac{1}{LC_i}\right) \\ + x_3\left(\frac{-(1-u)\,(c_1 + c_2)}{L}\right) + I_{pv}\left(-\frac{1}{C_i^2} - c_1 c_2 + \frac{1}{LC_i}\right) \\ + \dot{\hat{W}}^T \varphi\,(c_1 + c_2) - \ddot{\hat{W}}^T \varphi + \dot{V}_{pvr}\left(\frac{1}{C_i} + C_i c_1 c_2\right) \\ + \ddot{V}_{pvr}\,(C_i c_1 + C_i c_2) + C_i \ddot{V}_{pvr} \end{pmatrix}$$

By taking the time derivative of the Lyapunov function (32)

$$\dot{V} = Z_1\dot{Z}_1 + Z_2\dot{Z}_2 + Z_3\dot{Z}_3 - \tilde{W}^T P^{-1}\dot{\hat{W}} \tag{33}$$

By Substituting (16), (25) & (31) in (33) can be written as (34), shown at the bottom of the page, where c_3 is the gain constant

By solving $\dot{V}$, (35), as shown at the bottom of the page.

To obtain the asymptotically stable system, the above equation must be

$$\dot{V} = -c_1 Z_1^2 - c_2 Z_2^2 - c_3 Z_3^2$$

C. STEP 3: DETERMINING THE ONLINE WEIGHT UPDATE LAW

The final term in equation (35) must be equal to zero for making the system asymptotically stable.

$$\tilde{W}^T\left(P^{-1}\dot{\hat{W}} - \frac{\varphi Z_1}{C_i}\right) = 0$$

By solving the above equation

$$\dot{\hat{W}} = \frac{P\varphi Z_1}{C_i} \tag{36}$$

D. STEP 4: DETERMINING THE DUTY CYCLE

The second last term of (35) should need to be equal to zero in order to obtain the asymptotically stable system

$$-(1-u)\frac{Z_2}{L} + (1-u)\frac{x_2}{C} - \frac{x_3}{RC} - \dot{x}_{3d} + c_3 Z_3 = 0 \tag{37}$$

By substituting (11) and (22) in the above equation it can be rewritten as

$$-(1-u)\frac{(x_2 - x_{2d})}{L} + (1-u)\frac{x_2}{C} - \frac{x_3}{RC} - \dot{x}_{3d} + c_3(x_3 - x_{3d}) = 0 \tag{38}$$

By substituting (8), (28) and (31) in (38), (39) as shown at the bottom of the page.

Equation (39) can be rewritten as

$$a(1-u)^3 + b(1-u)^2 + c(1-u) + d = 0 \tag{40}$$

where

$$a = \frac{-1}{L}\left(x_2 - \hat{W}^T\varphi + C_i\dot{V}_{pvr} + \frac{x_2}{C} - C_i c_1\left(x_1 - V_{pvr}\right)\right)$$

$$b = x_3\left(c_1 + c_2 + c_3 - \frac{1}{RC}\right), \quad c = -LS_1 - c_3 LS_2$$

$$d = -L^2\dot{u}S_2$$

By solving for the cubic equation in (40) using Cardano formula and as $0 < u < 1$, the duty cycle is given by

$$u = \left(1 - \sqrt[3]{\left(q + \sqrt{q^2 + (r - p^2)^3}\right)} + \sqrt[3]{\left(q - \sqrt{q^2 + (r - p^2)^3}\right)} + p\right) \tag{41}$$

where

$$p = \frac{-b}{3a}, \quad q = p^3 + \frac{(bc - 3ad)}{6a^2} \text{ and } r = \frac{c}{3a}$$

Thus, the control law for the ABCNNC of the PV system is attained by cautiously selecting the values of c_1, c_2, c_3 and P. The gain constants c_1, c_2 and c_3 are influenced by the designer. However, larger value produces high overshoots henceforth for enhanced steady-state responses $c_1 > c_2 > c_3$. A larger range of P hints to a quicker response. Conversely, it reduces the stability margin. Hence, P must be within the range of 0 to 1 for the better transient response.

IV. STABILITY ANALYSIS

The stability exploration is achieved by commissioning the ABCNNC for the PV systems to find the adapted PV array voltage. In the following theorem, the Lyapunov stability property to track the desired PV array voltage is obtained and it is verified.

$$\dot{V} = \begin{pmatrix} Z_1\left(\frac{\tilde{W}^T\varphi}{C_i} - \frac{Z_2}{C_i} - c_1 Z_1\right) + Z_2\left(-(1-u)\frac{Z_3}{L} + \frac{Z_1}{C_i} - c_2 Z_2\right) + \\ + Z_3\left((1-u)\frac{x_2}{C} - \frac{x_3}{RC} - \dot{x}_{3d}\right) + c_3 Z_3^2 - c_3 Z_3^2 - \tilde{W}^T P^{-1}\dot{\hat{W}} \end{pmatrix} \tag{34}$$

$$\dot{V} = \begin{pmatrix} -c_1 Z_1^2 - c_2 Z_2^2 - c_3 Z_3^2 - \tilde{W}^T\left(P^{-1}\dot{\hat{W}} - \frac{\varphi Z_1}{C_i}\right) \\ + Z_3\left(-(1-u)\frac{Z_2}{L} + (1-u)\frac{x_2}{C} - \frac{x_3}{RC} - \dot{x}_{3d} + c_3 Z_3\right) \end{pmatrix} \tag{35}$$

$$\begin{pmatrix} (1-u)^3\left(\frac{-1}{L}\left(\begin{matrix} C_i\dot{V}_{pvr} + \frac{x_2}{C} - C_i c_1\left(x_1 - V_{pvr}\right) \\ + x_2 - \hat{W}^T\varphi \end{matrix}\right)\right) \\ + (1-u)^2\left(x_3\left(c_1 + c_2 + c_3 - \frac{1}{RC}\right)\right) + (1-u)\begin{pmatrix} -LS_1 \\ -c_3 LS_2 \end{pmatrix} \\ - L^2\dot{u}S_2 \end{pmatrix} = 0 \tag{39}$$

A. THEOREM

The duty cycle is shown in equation (41) and the online update law for the weights of the neural network specified in equation (36), confirms the confined approximation of changing PV current and asymptotically stable system for the closed-loop PV array while tracking the PV array voltage V_{pvr} i.e., $\lim_{t\to\infty} Z_1 = 0$ The error of the closed-loop strategies is ultimately bounded in the largest invariant set T.

B. PROOF

The closed-loop stability for the PV systems is examined by the error dynamics specified below

$$\begin{pmatrix}\dot{Z}_1\\ \dot{Z}_2\\ \dot{Z}_3\end{pmatrix} = \begin{pmatrix}-c_1 & \frac{-1}{C_i} & 0\\ \frac{1}{C_i} & -c_2 & \frac{-(1-u)}{L}\\ 0 & \frac{(1-u)}{L} & -c_3\end{pmatrix}\begin{pmatrix}Z_1\\ Z_2\\ Z_3\end{pmatrix} + \begin{pmatrix}\frac{\tilde{W}^T\varphi}{C_i}\\ 0\\ 0\end{pmatrix} \quad (42)$$

To investigate the stability, the error values had been described as $Z: = [Z_1\ Z_2\ Z_3]^T$ and the Lyapunov asymptotic stability function $V : F \subseteq R^7 x\,[0,\infty] \to R_+$ to be continuously differentiable and positive definite function and let $\mathcal{B}_n$ be the ball of radius n

$$V = \frac{1}{2}ZSZ^T + \frac{1}{2}\tilde{W}^T P^{-1}\tilde{W} \quad (43)$$

where P, S > 0. The class £ functions α_1 (•) and α_2 (•) exist and are defined on [0, n], where $\mathcal{B}_n \subset F \subseteq R^4\ X\ R^3$ such that

$$\alpha_1(\|\varsigma\|) \le V\left(Z,\ \tilde{W},\ t\right) \le \alpha_2(\|\varsigma\|) \quad \forall\varsigma \in \beta_n$$

where $\varsigma = \left[Z(t),\ \tilde{W}(t)\right]^T \in R^7$

By differentiating equation (43) and by substituting equation (42) produces

$$\dot{V} = \frac{1}{2}\left(\left(Z^T\left(SG + SG^T\right)Z\right) + \frac{1}{2}\left(\dot{\tilde{W}}^T P^{-1}\tilde{W}\right) + \frac{1}{2}\left(\tilde{W}^T P^{-1}\dot{\tilde{W}}\right)\right) + \begin{pmatrix}\frac{\tilde{W}^T\varphi}{C_i}\\ 0\\ 0\end{pmatrix} QZ \quad (44)$$

where $\left(G + G^T\right) = \begin{pmatrix}-c_1 & \frac{-1}{C_i} & 0\\ \frac{1}{C_i} & -c_2 & \frac{-(1-u)}{L}\\ 0 & \frac{(1-u)}{L} & -c_3\end{pmatrix}$

As P^{-1} a positive definite matrix and by assuming $S = I_{3\times3}$ and, equation (44) can be rewritten as

$$\dot{V} = \left(\frac{1}{2}\left(Z^T\left(G + G^T\right)Z\right) + \left(\tilde{W}^T P^{-1}\dot{\tilde{W}}\right) + \begin{pmatrix}\frac{\tilde{W}^T\varphi}{C_i}\\ 0\\ 0\end{pmatrix} Z\right) \quad (45)$$

By substituting the online weight update law equation (36), $\dot{V}$ can be written as

$$\dot{V} = \left(\frac{1}{2}\left(Z^T\left(G + G^T\right)Z\right)\right) = -Z^T YZ \le 0 \forall t \le 0, \quad \upsilon \in R^7 \quad (46)$$

where $-\frac{1}{2}\left(G + G^T\right) = Y$ is a symmetric matrix with positive values such that c_1, c_2, and $c_3 > 0$.

Hence the class £ functions α_3 (•) and α_4 (•) exists on [0, p] where $\mathcal{B}_p \subset F \subseteq R^3$ with the result

$$\alpha_3(\|Z\|) \le \dot{V}\left(Z, \tilde{W}, t\right) \le \alpha_4(\|Z\|) \quad \forall Z \in \beta_p \subset \beta_n \quad (47)$$

A compact invariant set $Y_1: = \{Z \in R^3: \dot{V} = 0 \Rightarrow Z = 0\}$ exists, and it becomes negative definite if the function falls outside Y_1. The Lyapunov function V: $[Z, \tilde{W}]^T \in R^7$ converges to T which is a large invariant set $T \subset Y_1$. In the large invariant set $Z = 0$ and $\dot{Z} = 0$ from that $\dot{\hat{W}} = 0$ and $\tilde{W}^T\varphi = 0\ \forall\,[Z, \hat{W}] \in T$. Since $Z_1 = x_1 - V_{pvr}$, then $x_1 = V_{pvr}$ and $\left(W - \hat{W}\right)^T[1 + \varphi(x_1) + \varphi(x_2) + \varphi(x_3)] = 0$, closed-loop strategies are eventually confined in the largest invariant set T. Thus the largest invariant set is $T \subset Y_1$ and which proves that $[Z, \hat{W}]$ converges to T proving $x_1 = V_{pvr}$ as $t \to \infty$. The Lyapunov control function V is radially unbounded and $\lim_{t\to\infty} V(t) = 0$, the Lyapunov function assures to be in £ L_∞ over the range from zero to infinity, for the ball of radius infinity (B_∞).

Hence the proposed ABCNNC for the PV systems is globally asymptotically stable over the region of attraction $Y_2 := \left\{\varsigma \in \alpha_\infty \backslash T : \dot{V} < 0\right\}$ for the class £ function $\alpha_\infty \subseteq F \subset R^4 x R^3$ as $n \to \infty$. Now for a change in current which is caused due to change in irradiance and temperature, the stability analysis has to be validated at different unknown time instances $T_n = [t_1, t_2, \ldots . t_n]$.

The Lyapunov function at these time instances is defined as

$$V = \frac{1}{2}Z_1 Z_1^T + \frac{1}{2}Z_2 Z_2^T + \frac{1}{2}Z_3 Z_3^T + \frac{1}{2}\tilde{W}^T P^{-1}\tilde{W}$$

For the system to be asymptotically stable based on equation (46), the derivative of the Lyapunov function $\dot{V}_n \le 0$. As V_n is positive definite, the Lyapunov function V_n decreases monotonically with respect to T_n. Based on the property of the Lyapunov function for $t_n < t_{n+1}$, the Lyapunov function becomes $V_n(t_n^+) = V_n(t_n) \ge V_n\left(t_{n+1}^-\right)$. During time t_0, the Lyapunov function will be $V_0(t_0^+) = V_0(t_0) \ge V_0\left(t_1^-\right)$.

Similarly, at time t_1 based on the property of Lyapunov function, it becomes $V_1\left(t_1^+\right) \leq 2V_0\left(t_1^-\right) + \nabla V_1$ for the change in solar current, where ∇V_1 is the result of variation in the solar current which will get implicated on the approximation function. Hence for the time t_{n+1} the Lyapunov function is $V_{n+1}\left(t_{n+1}^+\right) \leq 2V_n\left(t_{n+1}^-\right) + \nabla V_{n+1}$. Furthermore, for the next change, the Lyapunov function becomes

$$\begin{aligned} V_{n+1}\left(t_{n+1}^+\right) &\leq 2V_n\left(t_{n+1}^-\right) + \nabla V_{n+1} \\ &\leq 4V_{n-1}\left(t_n^-\right) + 2\nabla V_n + \nabla V_{n+1} \end{aligned}$$

Hence by a repetitive procedure, the final Lyapunov control function is $V_{n+1}(t_{n+1}) \leq \partial V_0(t_0) + \varepsilon$ for $t \in [t_{n+1}, \infty]$, where ∂ and ε are the positive constants. As $V_0(t_0)$ is bounded for the subsequent change in solar current, hence the system is bounded which enumerates the proposed controller is globally asymptotically stable for change in uncertainty.

V. SIMULATION RESULTS AND DISCUSSIONS

The ABCNNC is proposed for the solar panels to extract the maximum power by tracking the desired PV voltage which is obtained by the linear regression method. The desired PV voltage is found by the control law attained from equation (41) for the proposed controller. The PV system is simulated keeping the step size as 1 μs in the MATLAB by means of PV parameters, boost converter parameters and controller parameters as stated in Tables 1 and 2. To get the enhanced static and dynamic responses the gain constants c_1, c_2 and c_3 and the adaptation rate P have to be carefully selected. The simulated responses of the PV array voltage, PV power, boost converter inductor current, boost converter output voltage and the power across the load are recorded. The accomplishment of the ABCNNC is endorsed from the simulation results by analogizing it with the constant voltage PID controller and Back Stepping Controller (BSC). The proportional gain (K_p), Integral gain (K_i), derivative gain (K_d) and filter coefficient of the PID controller are -0.0943, -3.138, -0.000702 and 7542.55 respectively. The proposed ABCNNC is simulated for the comprehensive range of variation in the irradiance, temperature and load resistance in the following seven case studies to show the robustness which makes its compatibility in real-time.

TABLE 2. Boost converter and controller parameters.

Boost Converter Parameters	Simulation Value	Experimental Value
Output capacitance C	320 μ F	470 μ F
Boost Inductor L	10 mH	10 mH
Input capacitance C_i	220 μ F	220 μ F
Load Resistance R	30 Ω	15 Ω
Controller Parameters	**Simulation Value**	**Experimental Value**
Gain constant c_1	$1e^6$	$1e^5$
Gain constant c_2	$1e^5$	$1e^4$
Gain constant c_3	$1e^4$	$1e^3$
Adaptation rate P	$1e^{-27}$	$1e^{-27}$
Positive Scalar constant k_w	$10e^{24}$	$10e^{24}$
Number of neurons n	5	5

A. CASE 1: STARTUP RESPONSE

In this case study, the start-up response of the proposed Chebyshev neural network controller, backstepping controller and constant voltage PID controller are attained from the parameters mentioned in Tables 1 and 2. The simulated responses of the solar panel voltage, solar input power, boost converter inductor current, boost converter load voltage, the power across the load and the estimation of CNN are obtained for all three controllers and are shown in figure 6. It is apparent from figure 6, that the maximum power is extracted by obtaining the desired PV array voltage for the proposed ABCNNC with minimum overshoot (M_p), less settling time (t_s) and rise time (t_r). Based on the waveforms of the solar panel output voltage, inductor current and boost converter load voltage, it is identified that the ABCNNC displays enriched steady-state and transient responses and its particulars are enumerated in table 3. The settling time of the PV Voltage is decreased by 68.7 % and 1% in comparison with the constant voltage PID controller and BSC. Likewise, the settling time of the inductor current is reduced by 57.7 % and 43.76 % and the settling time of boost converter output voltage is lessened by 66.1 % and 26.64 % in assessment with the constant voltage PID controller and BSC respectively. The peak overshoot of the PV voltage for the ABCNNC is 40.134 V which is 4.922 V and 2.064 V less in comparison with constant voltage PID controller and BSC respectively.

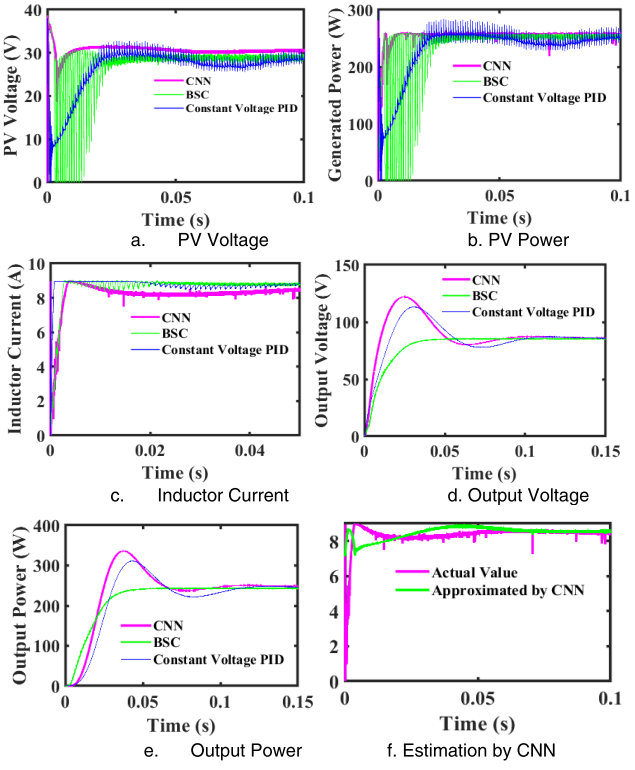

FIGURE 6. Startup responses of the proposed CNN, BSC and constant voltage PID.

TABLE 3. Start-up responses of the solar panel voltage, boost converter current and output load voltage.

Parameter	Controller	Performance		
		t_r (ms)	t_s (ms)	Over shoot %
PV Voltage	Constant Voltage PID	0.002733	38.3	47.725
	BSC	0.00260	21.6	38.3552
	ABCNNC	**0.002703**	**12**	**31.59**
Inductor Current	Constant Voltage PID	0.00167	480	5.9316
	BSC	0.0007046	361	5.15
	ABCNNC	**0.0001523**	**203**	**2.8032**
Output Voltage	Constant Voltage PID	47.4	59.3	0.1048
	BSC	18.9	27.4	0.5159
	ABCNNC	**13.4**	**20.1**	**0.3658**

B. CASE 2: CHANGE IN IRRADIANCE FROM 1000 W/m^2 TO 800 W/m^2

In this case at constant temperature 25°C, the irradiance is reduced to 800 W/m^2 from 1000 W/m^2 at time t = 0.5 s. The simulated responses of the solar panel voltage, solar input power, boost converter inductor current, boost converter load voltage, the power across the load and the estimation of CNN are shown in figure 7. Because of the implementation of CNN in the proposed controller, the weights are tuned quickly which will produce the impact on the duty cycle equation where it is being computed swiftly for the change in uncertainties caused by irradiance in accordance with the BSC and constant voltage PID controller and the particulars are shown in table 4. From table 4, it is evident for the proposed controller that the settling time of the PV voltage is decreased

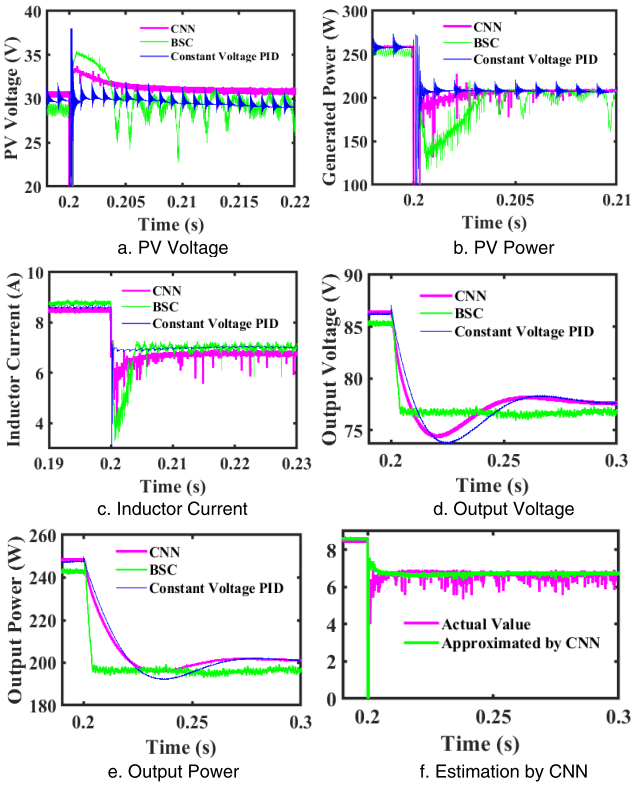

FIGURE 7. Responses of the proposed CNN, BSC and constant voltage PID for change in irradiance to 800 W/m^2 from 1000 W/m^2.

TABLE 4. Responses of the solar panel voltage, boost converter current and output load voltage for case 2.

Parameter	Controller	Performance		
		t_r (ms)	t_s (ms)	Over shoot %
PV Voltage	Constant Voltage PID	0.144	12.4	87.58
	BSC	0.266	3	11.02
	ABCNNC	**0.0325**	**2**	**8.567**
Inductor Current	Constant Voltage PID	0	54.5	7.166
	BSC	0	5	0
	ABCNNC	**0**	**4**	**0**
Output Voltage	Constant Voltage PID	14.7	24.1	12.16
	BSC	14.1	21.6	13.52
	ABCNNC	**11.5**	**18.9**	**11.357**

by 10.4 ms and 1 ms in comparison with the constant voltage PID controller and BSC. Likewise, the settling time of the boost converter inductor current and boost converter load voltage for the proposed controller is considerably reduced in assessment with constant voltage PID controller and BSC. The peak overshoot is reduced significantly in the proposed controller for the decrease in irradiance in comparison with the other two controllers.

C. CASE 3: CHANGE IN IRRADIANCE FROM 800 W/m^2 TO 1200 W/m^2

To investigate the robustness of the proposed control technique over a wide range of operating points, the PV array is subjected to the sudden increase in irradiance from 800 W/m^2 to 1200 W/m^2 at time t = 1 second. The obtained responses of all three controllers during such large uncertainty are shown in figure 8. The uncertainties caused by the change in irradiance are eluded quickly by the use of the weight update law of the CNN in the ABCNNC for the uncertainties. Hence, by the implementation of CNN, the settling time of the PV voltage, inductor current and boost converter output voltage is decreased significantly.

It is obvious from figure 8, that ABCNNC takes less time to reach the desired value of PV voltage, inductor current and boost converter output load voltage in comparison with constant voltage PID controller and conventional backstepping technique and is given in table 5. It is apparent from the table that for the change in irradiance, the ABCNNC tracks the desired PV voltage in 5 ms which is 90.11 % and 75.37 % less in comparison with constant voltage PID controller and BSC respectively. Likewise, in the ABCNNC for the inductor current and boost converter output load voltage, it is apparent that the time taken to reach desired value is reduced significantly in evaluation with constant voltage PID controller and BSC. The peak overshoot is reduced to 16.41 % which is 81.89 % and 0.07% less in accordance with the constant voltage PID controller and BSC.

D. CASE 4: CHANGE IN TEMPERATURE FROM 25°C TO 40°C

To investigate the robustness of the proposed control technique over a wide range of temperature, the PV panel is

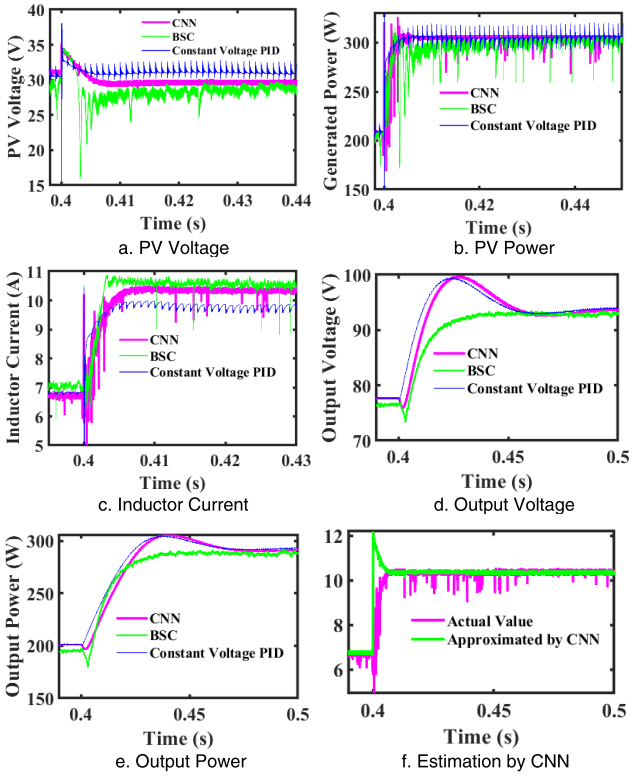

FIGURE 8. Responses of the proposed CNN, BSC and constant voltage PID for change in irradiance to 1200 W/m^2 from 800 W/m^2.

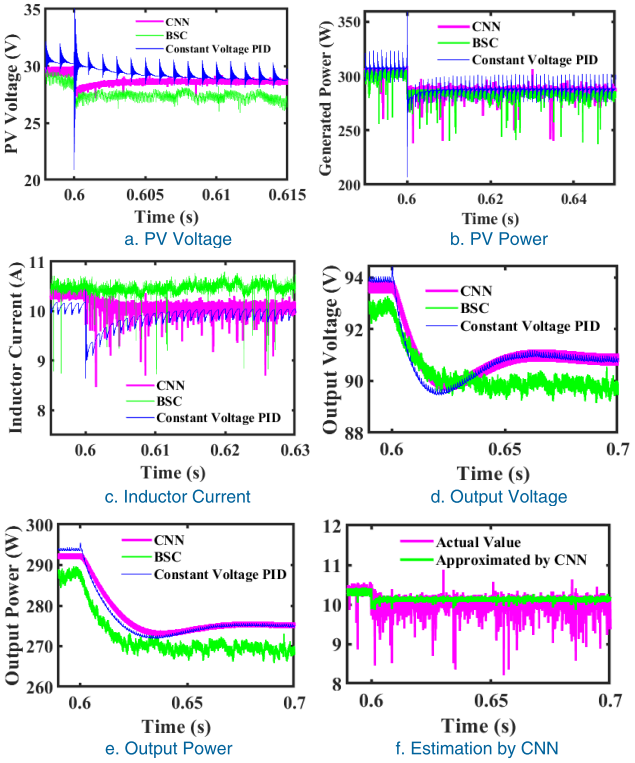

FIGURE 9. Responses of the proposed CNN, BSC and constant voltage PID for change in temperature to 40°C from 25°C.

TABLE 5. Responses of the solar panel voltage, boost converter current and output load voltage for case 3.

Parameter	Controller	Performance	
		t_s (ms)	Over shoot %
PV Voltage	Constant Voltage PID	50.6	93.323
	BSC	20.3	17.7961
	ABCNNC	**5**	**16.41**
Inductor Current	Constant Voltage PID	55.1	3.4409
	BSC	22.47	3.3892
	ABCNNC	**5.19**	**2.7309**
Output Voltage	Constant Voltage PID	57.76	0.0455
	BSC	30.13	0.3102
	ABCNNC	**15.2**	**0.0074**

TABLE 6. Responses of the solar panel voltage, boost converter current and output load voltage for case 4.

Parameter	Controller	Performance	
		t_s (ms)	Over shoot %
PV Voltage	Constant Voltage PID	6	20.7997
	BSC	**4.8**	**4.8287**
	ABCNNC	**3.91**	**5.9956**
Inductor Current	Constant Voltage PID	9	0
	BSC	**7.65**	**3.2821**
	ABCNNC	**2.3**	**14.0093**
Output Voltage	Constant Voltage PID	6.2	4.0287
	BSC	10	3.5430
	ABCNNC	**5**	**3.5857**

subjected to a sudden increase in temperature from 25°C to 40°C at time t = 0.6 seconds. The obtained responses of all three controllers during increase in temperature are shown in figure 9. The uncertainties caused by the change in temperature are eluded quickly by the use of the weight update law of CNN in the ABCNNC and the obtained results are shown in table 6. Hence by the implementation of CNN, the settling time and overshoot of the PV voltage, inductor current and output voltage is decreased significantly. It is obvious from figure 9, that the ABCNNC takes less time in obtaining the desired value of PV voltage, inductor current and output voltage in comparison with the constant voltage PID controller and conventional backstepping technique and is given in table 6. It is obvious from the table that for the variation in torque load, the ABCNNC tracks the PV voltage in 3.91 ms that is found to be 34.83 % and 18.54 % less in comparison with constant voltage PID controller and BSC respectively. Likewise in the ABCNNC for the inductor current and output voltage, it is apparent that the ABCNNC requires minimum time for obtaining the desired value in evaluation with the constant voltage PID controller and BSC.

E. CASE 5: CHANGE IN TEMPERATURE FROM 40°C TO 30°C

In this case, the temperature is decreased to 25°C from 40°C at time t = 0.8 seconds. Figure 10 shows the responses obtained by the controllers for this case study. From these figures, it is clear that the proposed ABCNNC shows enhanced

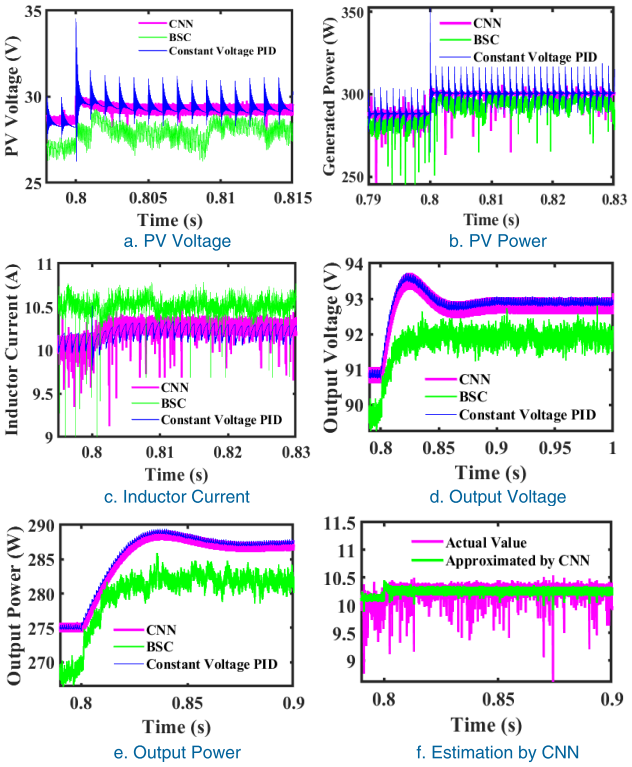

FIGURE 10. Responses of the proposed CNN, BSC and constant voltage PID for change in temperature to 30° C from 40°C.

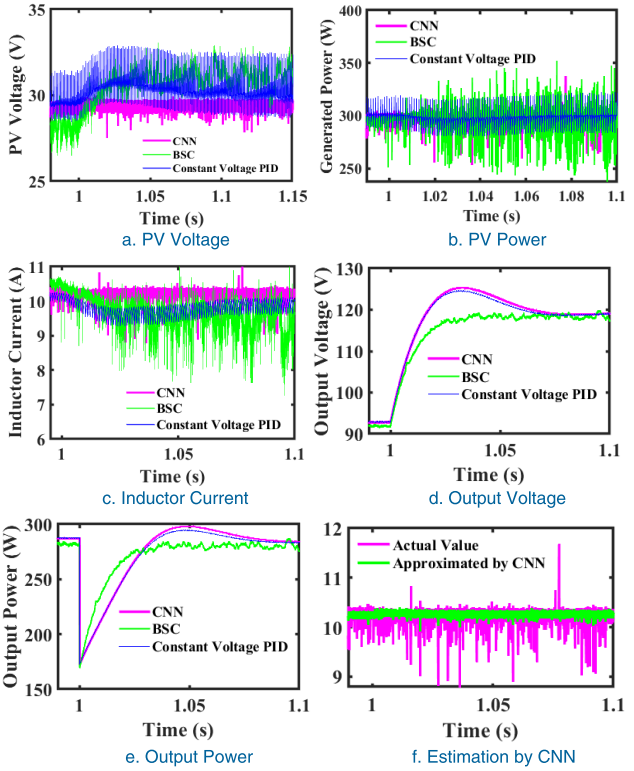

FIGURE 11. Responses of the proposed CNN, BSC and constant voltage PID for change in load resistance to 50 Ω from 30 Ω.

TABLE 7. Responses of the solar panel voltage, boost converter current and output load voltage for case 5.

Parameter	Controller	Performance	
		t_s (ms)	Over shoot %
PV Voltage	Constant Voltage PID	**2.6**	**17.3472**
	BSC	10.3	4.0880
	ABCNNC	**2.2**	**1.8786**
Inductor Current	Constant Voltage PID	**3.8**	**2.8003**
	BSC	12.2	6.3737
	ABCNNC	**2.658**	**3.5634**
Output Voltage	Constant Voltage PID	**25**	**0.9536**
	BSC	16	0.9155
	ABCNNC	**6**	**0.7534**

TABLE 8. Responses of the solar panel voltage, boost converter current and output load voltage for case 6.

Parameter	Controller	Performance	
		t_s (ms)	Over shoot %
PV Voltage	Constant Voltage PID	12.3	11.3869
	BSC	10.67	7.4387
	ABCNNC	**3.53**	**1.3479**
Inductor Current	Constant Voltage PID	6.74	0.4719
	BSC	9.83	15.3144
	ABCNNC	**4.47**	**14.7071**
Output Voltage	Constant Voltage PID	33	4.4603
	BSC	9	1.3618
	ABCNNC	**5**	**4.8891**

transient performance. Table 7 gives the observed settling times and peak overshoot of PV voltage, inductor current and output voltage. For the PV voltage, the settling time is 2.2 ms which is a much lesser time in contrast to the constant voltage PID controller and BSC as given in table 7.

F. CASE 6: CHANGE IN RESISTANCE FROM 30Ω TO 50 Ω

Next, to analyze the suitability of solar panels for the transition of load resistance from the lower value to a higher value, the load resistance is varied from 30 Ω to 50 Ω at time t = 1 seconds and its responses are shown in figure 11. Because of the implementation of CNN in the proposed controller, the weights are tuned quickly which will produce the impact on the duty cycle equation where it is being computed swiftly for the change in uncertainties caused by load resistance in accordance with the BSC and PID controller and the particulars are listed in table 8. It is evident from Table 8 that for the increase in load resistance, the ABCNNC quickly tracks the desired PV voltage in much lesser time as compared with other two controllers.

G. CASE 7 CHANGE IN RESISTANCE FROM 50Ω TO 20Ω

In this case, the load resistance is reduced from 50 Ω to 20 Ω at time t = 1.2 seconds. Figure 12 displays the responses attained by the three controllers for the decrease in load resistance. From these figures, it is vibrant that the ABCNNC

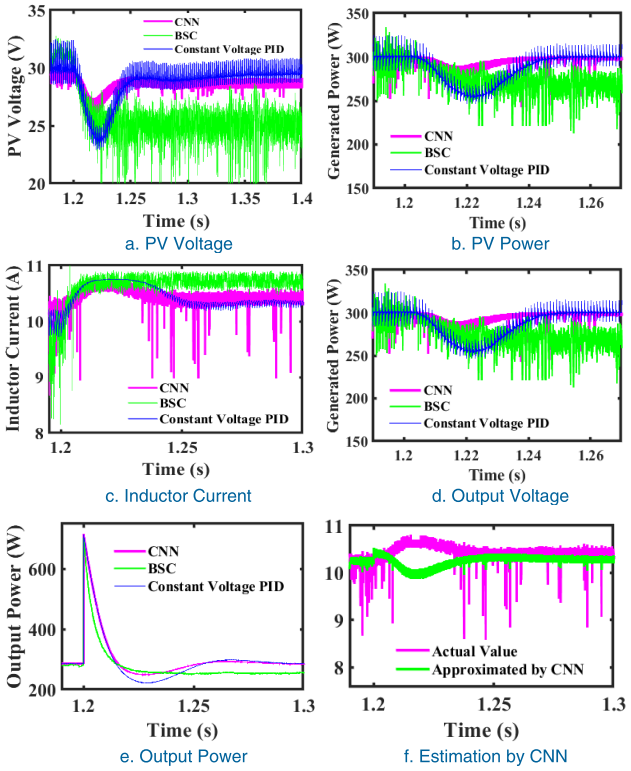

FIGURE 12. Responses of the proposed CNN, BSC and constant voltage PID for change in load resistance to 20 Ω from 50 Ω.

TABLE 9. Responses of the solar panel voltage, boost converter current and output load voltage for case 7.

Parameter	Controller	Performance	
		t_s (ms)	Over shoot %
PV Voltage	Constant Voltage PID	43	6.8527
	BSC	36	30.2833
	ABCNNC	**17.8**	**2.0282**
Inductor Current	Constant Voltage PID	49	5.5818
	BSC	31.27	3.2064
	ABCNNC	**11.93**	**10.8032**
Output Voltage	Constant Voltage PID	9.7	57.0375
	BSC	5.67	65.5231
	ABCNNC	**4.78**	**57.6988**

displays enriched transient performance. The particulars are given in table 9.

From table 9, it is clear that for the decline in load resistance, the proposed controller is found to achieve the desired trajectory at 17.8 ms which is comparatively faster than the constant voltage PID controller and BSC. The corresponding inductor current and output voltage also witnesses a quicker adaptation with the proposed control technique.

VI. EXPERIMENTAL RESULTS AND DISCUSSIONS

The ABCNNC is proposed for the solar panels to extract the maximum power by tracking the desired PV voltage obtained by the linear regression method. The PV voltage is found by the control law attained from equation (41) for the proposed controller. A model for the implementation of ABCNNC in the photo voltaic system to extract the maximum power is designed in the laboratory and the prototype is shown in figure 13. The prototype is designed by the PV parameters, boost converter parameters and controller parameters as stated in tables 1 and 2. To get the enhanced static and dynamic responses, the gain constants c_1, c_2, c_3, and the adaptation rate P have to be carefully selected. The duty cycle of the proposed controller is obtained by sensing the current and voltage across the solar panel, inductor and load. Based on the duty cycle, the gate pulses will be generated and fed to the MOSFET which will control the PV voltage and output voltage. In the prototype ARM LPC 2148, a 32-bit processor is used as a controller to sense the voltage and current and to produce the gate pulses based on the duty cycle obtained from the PV voltage, PV current, inductor current, and output load voltage. LPC 2148 has a 10-bit resolution inbuilt DAC and ADC of 3.3 V range. The amplitude of the generated gate pulses is 3.3 V which is not sufficient to drive the IRFP460 MOSFET it needs 12 V to drive it. To drive the MOSFET a gate driver circuit is designed using IR2110 driver IC, UF4007 diode, 10 KΩ, and 1 KΩ resistances, and 22 μF and 100 nF capacitances. IC HPCL 2611 optocoupler is used to separate the PV system from the controlling circuit. The current of the PV panels and the inductor is sensed using ACS – 312T (0 – 20 A). The voltage across the PV panels and load is measured using (0 – 100 V) sensor which is designed by connecting 220 KΩ and 7.5 KΩ in series and measuring the sensed voltage across 7.5 KΩ which is of (0 – 3.3 V) range. The responses of the PV voltage, PV power, boost converter current, boost converter voltage, and the power across the load is recorded. The accomplishment of the ABCNNC is endorsed from the recorded results by analogizing it with the constant voltage PID controller and BSC.

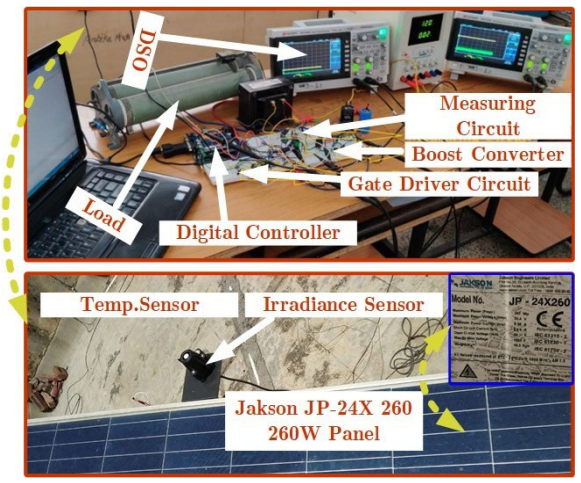

FIGURE 13. Experimental set up of the proposed controller for the PV system.

A. TRANSIENT PERFORMANCE ANALYSIS

The response of the Chebyshev neural network controller, backstepping controller, and constant voltage PID controller are attained from the parameters mentioned in tables 1 and 2.

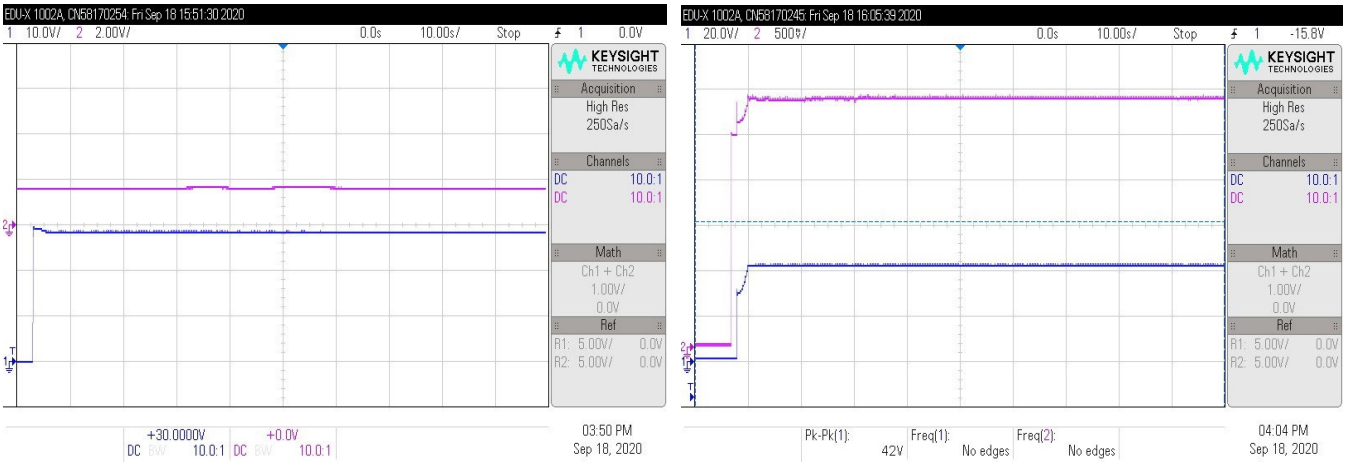

a. Irradiance and PV voltage

b. PV Current and output voltage

FIGURE 14. **Responses of proposed controller.**

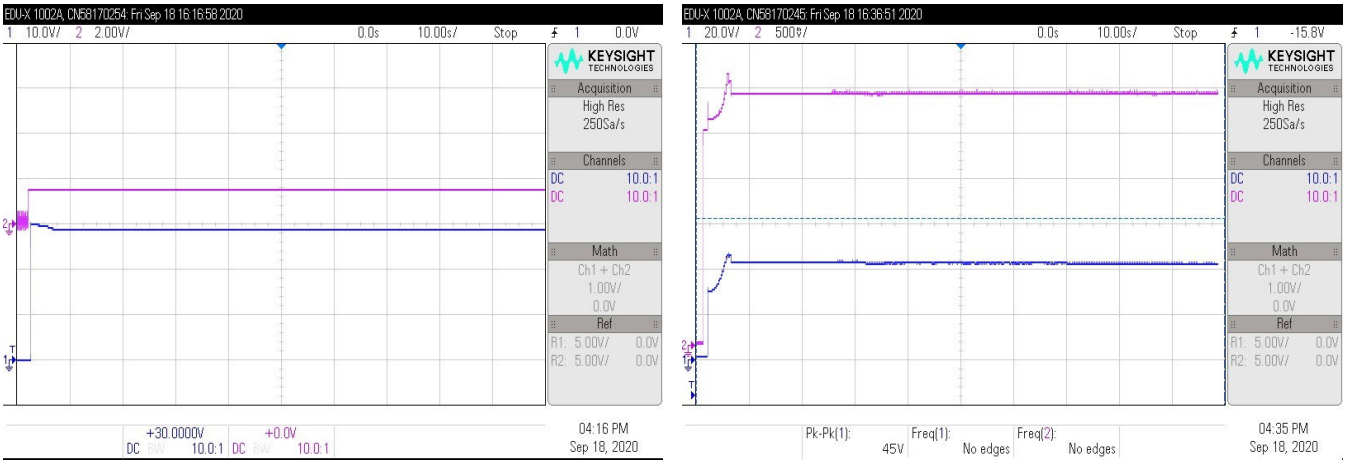

a. Irradiance and PV voltage

b. PV Current and output voltage

FIGURE 15. **Responses of BSC controller.**

The obtained responses of the solar panel voltage, solar input power, boost converter inductor current, boost converter load voltage, and the power across the load is obtained for all three controllers and are shown in figures 14, 15 and 16.

It is apparent from figures 14, 15 and 16 that the maximum power is obtained by attaining the desired solar panel voltage for the proposed ABCNNC with M_p, less settling time t_s and rise time t_r. Based on the waveforms of the solar panel voltage, inductor current, and load voltage, it is identified that the ABCNNC displays enriched steady-state and transient responses and its particulars are enumerated in table 10.

The t_s of the PV voltage are decreased by 53.67 % and 50.75 % in comparison with the constant voltage PID controller and BSC. Likewise, the settling time of the output load voltage is reduced by 46.7 5 % and 34.77 % in assessment with the constant voltage PID controller and BSC respectively. The peak overshoot of the PV voltage for the ABCNNC is less in comparison with the constant voltage PID controller and BSC.

TABLE 10. **Transient performance evaluation of the PV array voltage and output load voltage.**

Parameter	Controller	Performance		
		t_r (s)	t_s (s)	Over shoot %
PV Voltage	Constant Voltage PID	0.065	3.75	3.23
	BSC	0.039	3.582	3.846
	ABCNNC	**0.062**	**1.764**	**3.448**
Output Voltage	Constant Voltage PID	2.77	4.01	10.43
	BSC	2.77	3.274	1.39
	ABCNNC	**1.813**	**2.135**	**1.32**

The efficiency of the proposed controller in terms of maximum power is defined as

$$\eta = \frac{P_{avg}}{P_{max\,r}} x\,100 \tag{48}$$

where P_{avg} is the average power obtained from the solar panel and Pmaxr is the reference maximum power obtained

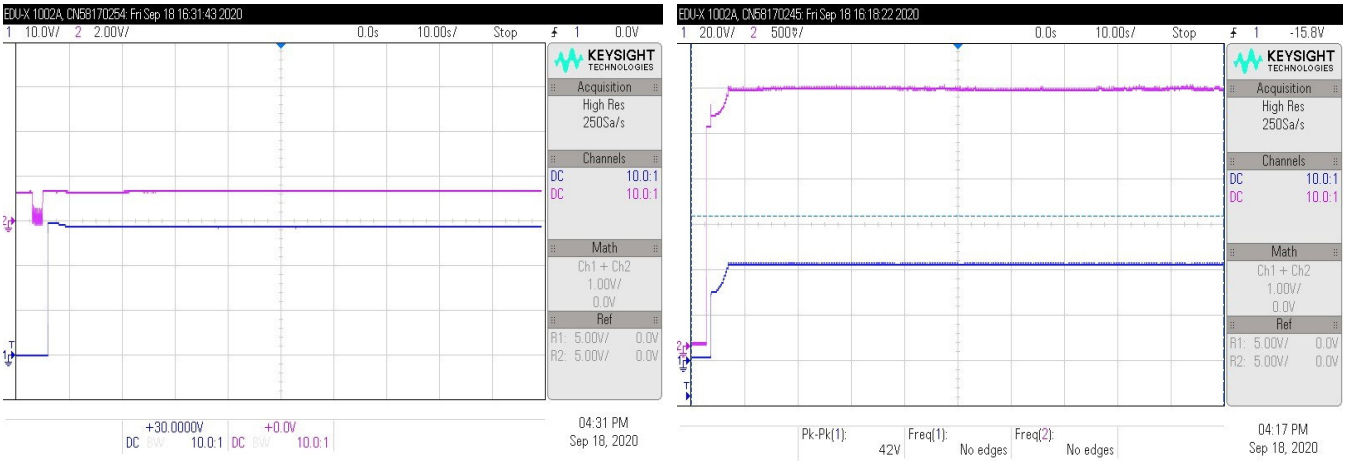

a. Irradiance and PV voltage

b. PV Current and output voltage

FIGURE 16. Responses of PID controller.

TABLE 11. Maximum power point tracking efficiency.

Controller	Irradiance (W/m^2)/ Temperature (°C)	Pmaxr (W)	Efficiency (η) (%)
Constant Voltage PID	473.1588 / 31	128.65	97.100
BSC	551.81 / 31	142.70	98.010
ABCNNC	**582.57 / 31**	**150.17**	**99.78**

from equation 5 for the given irradiance and temperature. The details of the efficiency obtained by equation 48 for the different controllers are given in table 11. From the table, it is evident that the proposed controller extracts the desired maximum power with maximum efficiency.

B. DYNAMIC PERFORMANCE ANALYSIS

The dynamic analysis of the ABCNNC is examined by Integral Time Square Error (ITSE), Integral Square Error (ISE), Integral Time Absolute Error (ITAE), Integral Absolute Error (IAE) and Mean Relative Error (MRE) in assessment with constant voltage PID controller and backstepping controller and their particulars are tabulated in table 12. From table 12, it is understood that ABCNNC indicates the least error indices evaluation with constant voltage PID controller and backstepping controller, which confirms the improved performance of ABCNNC. Further, the efficiency of the proposed technique is compared with existing techniques presented in literature and it is confirming that the proposed technique has low settling time with maximum efficiency of 99.78% as shown in table 13.

TABLE 12. Dynamic analysis of the proposed CNN controller, conventional backstepping controller, and constant voltage PID controller.

Controller	MRE	IAE	ITAE	ISE	ITSE
Constant Voltage PID	0.015	55.02	1266.9	137.68	1293.5
BSC	0.012	22.91	211.22	59.21	178.77
ABCNNC	**0.002**	**18.24**	**193.07**	**57.94**	**174.46**

TABLE 13. Comparison of experimental efficiency of various techniques.

Ref	Power (W)	t_s (s)	Efficiency (%)
[7]	240	~ (5 - 6)	99.00
[9]	60.0	~1.8	92.00
[13]	16.6	20.2	96.00
[15]	125.0	~ (20 – 24)	80.00
Proposed (ABCNNC)	**260.0**	**1.764**	**99.78**

VII. CONCLUSION

In this work, an adaptive Chebyshev neural backstepping controller is proposed to extract the maximum power from the solar panel and implemented in simulation and real-time. Chebyshev polynomials are used to approximate the fluctuating PV current which is caused due to change in irradiance and temperature in the proposed controller. Because of the orthogonal property and its ability to conserve power series, Chebyshev polynomials approximate the varying PV current by tuning the controller to the desired reference voltage in quick time. The desired reference voltage to extract the maximum power is obtained by the linear regression method. ABCNNC improved the transient and dynamic performances of the PV system besides the approximation. The proposed controller is tested in different operating conditions. Simulation and experimental results are taken at different irradiance, temperature and load resistance with the proposed controller and are compared with the BSC and constant voltage PID to show the effective performance of the proposed controller. Assessment of results with the BSC and constant voltage PID shows enhanced steady-state and transient responses in simulation and real-time. Henceforth for any type of disturbances caused by the environment to the PV panel, the proposed controller is found to be more efficient in getting the maximum power.

VIII. FUTURE WORK

The linear regression method generates the reference voltage based on the irradiance and temperature for the entire PV cells. But, under shading conditions the irradiance is different for each PV cells depending upon the shading. Hence the ability to attain the reference PV voltage using linear regression method in the proposed controller is degraded. Thus, the proposed controller shows less efficiency in drawing maximum power under shading / partial shading conditions. In future, this issue could be alleviated by incorporating appropriate method to find the desired reference voltage under shading conditions using this proposed controller. The proposed controller can be designed for solar-powered PMDC applications such as electric vehicles and agricultural pumps.

REFERENCES

[1] F. Dinçer, "The analysis on photovoltaic electricity generation status, potential and policies of the leading countries in solar energy," *Renew. Sustain. Energy Rev.*, vol. 15, no. 1, pp. 713–720, Jan. 2011.

[2] H. X. Li, D. J. Edwards, M. R. Hosseini, and G. P. Costin, "A review on renewable energy transition in australia: An updated depiction," *J. Cleaner Prod.*, vol. 242, Jan. 2020, Art. no. 118475.

[3] L. Cheng, F. Zhang, S. Li, J. Mao, H. Xu, W. Ju, X. Liu, J. Wu, K. Min, X. Zhang, and M. Li, "Solar energy potential of urban buildings in 10 cities of China," *Energy*, vol. 196, Apr. 2020, Art. no. 117038.

[4] T. V. Dixit, A. Yadav, and S. Gupta, "Experimental assessment of maximum power extraction from solar panel with different converter topologies," *Int. Trans. Electr. Energy Syst.*, vol. 29, no. 2, p. e2712, Feb. 2019.

[5] M. H. Taghvaee, M. A. M. Radzi, S. M. Moosavain, H. Hizam, and M. H. Marhaban, "A current and future study on non-isolated DC-DC converters for photovoltaic applications," *Renew. Sustain. Energy Rev.*, vol. 17, pp. 216–227, 2013.

[6] S. K. Kollimalla and M. K. Mishra, "A novel adaptive P&O MPPT algorithm considering sudden changes in the irradiance," *IEEE Trans. Energy Convers.*, vol. 29, no. 3, pp. 602–610, Sep. 2014.

[7] J. Ahmed and Z. Salam, "An enhanced adaptive P&O MPPT for fast and efficient tracking under varying environmental conditions," *IEEE Trans. Sustain. Energy*, vol. 9, no. 3, pp. 1487–1496, Jul. 2018.

[8] H. H. H. Mousa, A.-R. Youssef, and E. E. M. Mohamed, "Variable step size P&O MPPT algorithm for optimal power extraction of multi-phase PMSG based wind generation system," *Int. J. Electr. Power Energy Syst.*, vol. 108, pp. 218–231, Jun. 2019.

[9] K. S. Tey and S. Mekhilef, "Modified incremental conductance algorithm for photovoltaic system under partial shading conditions and load variation," *IEEE Trans. Ind. Electron.*, vol. 61, no. 10, pp. 5384–5392, Oct. 2014.

[10] H. Shahid, M. Kamran, Z. Mehmood, M. Y. Saleem, M. Mudassar, and K. Haider, "Implementation of the novel temperature controller and incremental conductance MPPT algorithm for indoor photovoltaic system," *Sol. Energy*, vol. 163, pp. 235–242, Mar. 2018.

[11] T. Esram, J. W. Kimball, P. T. Krein, P. L. Chapman, and P. Midya, "Dynamic maximum power point tracking of photovoltaic arrays using ripple correlation control," *IEEE Trans. Power Electron.*, vol. 21, no. 5, pp. 1282–1290, Sep. 2006.

[12] C. Barth and R. C. N. Pilawa-Podgurski, "Dithering digital ripple correlation control for photovoltaic maximum power point tracking," *IEEE Trans. Power Electron.*, vol. 30, no. 8, pp. 4548–4559, Aug. 2015.

[13] L. M. Elobaid, A. K. Abdelsalam, and E. E. Zakzouk, "Artificial neural network-based photovoltaic maximum power point tracking techniques: A survey," *IET Renew. Power Gener.*, vol. 9, no. 8, pp. 1043–1063, 2015.

[14] A. M. Kassem, "MPPT control design and performance improvements of a PV generator powered DC motor-pump system based on artificial neural networks," *Int. J. Electr. Power Energy Syst.*, vol. 43, no. 1, pp. 90–98, Dec. 2012.

[15] A. El Khateb, N. A. Rahim, J. Selvaraj, and M. N. Uddin, "Fuzzy-logic-controller-based SEPIC converter for maximum power point tracking," *IEEE Trans. Ind. Appl.*, vol. 50, no. 4, pp. 2349–2358, Jul./Aug. 2014.

[16] S. Farajdadian and S. M. H. Hosseini, "Design of an optimal fuzzy controller to obtain maximum power in solar power generation system," *Sol. Energy*, vol. 182, pp. 161–178, Apr. 2019.

[17] B. Yang, T. Yu, H. Shu, D. Zhu, N. An, Y. Sang, and L. Jiang, "Energy reshaping based passive fractional-order PID control design and implementation of a grid-connected PV inverter for MPPT using grouped grey wolf optimizer," *Sol. Energy*, vol. 170, pp. 31–46, Aug. 2018.

[18] A. I. Dounis, P. Kofinas, C. Alafodimos, and D. Tseles, "Adaptive fuzzy gain scheduling PID controller for maximum power point tracking of photovoltaic system," *Renew. Energy*, vol. 60, pp. 202–214, Dec. 2013.

[19] Z. Ye and X. Wu, "Compensation loop design of a photovoltaic system based on constant voltage MPPT," in *Proc. Asia–Pacific Power Energy Eng. Conf.*, Mar. 2009, pp. 1–4.

[20] S.-I. Go, S.-J. Ahn, J.-H. Choi, W.-W. Jung, S.-Y. Yun, and I.-K. Song, "Simulation and analysis of existing MPPT control methods in a PV generation system," *J. Int. Council Electr. Eng.*, vol. 1, no. 4, pp. 446–451, Oct. 2011.

[21] H. A. Mohamed-Kazim, I. Abdel-Qader, and A. M. Harb, "Efficient maximum power point tracking based on reweighted zero-attracting variable stepsize for grid interfaced photovoltaic systems," *Comput. Electr. Eng.*, vol. 85, Jul. 2020, Art. no. 106672.

[22] M. A. Mahmud, M. J. Hossain, H. R. Pota, and N. K. Roy, "Robust nonlinear controller design for three-phase grid-connected photovoltaic systems under structured uncertainties," *IEEE Trans. Power Del.*, vol. 29, no. 3, pp. 1221–1230, Jun. 2014.

[23] Y. Levron and D. Shmilovitz, "Maximum power point tracking employing sliding mode control," *IEEE Trans. Circuits Syst. I, Reg. Papers*, vol. 60, no. 3, pp. 724–732, Mar. 2013.

[24] C.-S. Chiu, Y.-L. Ouyang, and C.-Y. Ku, "Terminal sliding mode control for maximum power point tracking of photovoltaic power generation systems," *Sol. Energy*, vol. 86, no. 10, pp. 2986–2995, Oct. 2012.

[25] T. F. Orchi, T. K. Roy, M. A. Mahmud, and A. M. T. Oo, "Feedback linearizing model predictive excitation controller design for multimachine power systems," *IEEE Access*, vol. 6, pp. 2310–2319, 2018.

[26] S. Ma, M. Chen, J. Wu, W. Huo, and L. Huang, "Augmented nonlinear controller for maximum power-point tracking with artificial neural network in grid-connected photovoltaic systems," *Energies*, vol. 9, no. 12, p. 1005, Nov. 2016.

[27] A. Lashab, D. Sera, and J. M. Guerrero, "A dual-discrete model predictive control-based MPPT for PV systems," *IEEE Trans. Power Electron.*, vol. 34, no. 10, pp. 9686–9697, Oct. 2019.

[28] B. Laxmidhar and K. Indrani, *Intelligent Control Systems: Principles and Applications*. New Delhi, India: Oxford Univ. Press, 2009.

[29] H. Armghan, M. Yang, M. Q. Wang, N. Ali, and A. Armghan, "Nonlinear integral backstepping based control of a DC microgrid with renewable generation and energy storage systems," *Int. J. Electr. Power Energy Syst.*, vol. 117, May 2020, Art. no. 105613.

[30] M. Arsalan, R. Iftikhar, I. Ahmad, A. Hasan, K. Sabahat, and A. Javeria, "MPPT for photovoltaic system using nonlinear backstepping controller with integral action," *Sol. Energy*, vol. 170, pp. 192–200, Aug. 2018.

[31] T. K. Roy and M. A. Mahmud, "Active power control of three-phase grid-connected solar PV systems using a robust nonlinear adaptive backstepping approach," *Sol. Energy*, vol. 153, pp. 64–76, Sep. 2017.

[32] H. Armghan, I. Ahmad, A. Armghan, S. Khan, and M. Arsalan, "Backstepping based non-linear control for maximum power point tracking in photovoltaic system," *Sol. Energy*, vol. 159, pp. 134–141, Jan. 2018.

[33] Q. Hou, J. Dong, and C. Xi, "Adaptive neural network tracking control for switched uncertain non-linear systems with actuator failures and time-varying delays," *IET Control Theory Appl.*, vol. 13, no. 12, pp. 1929–1939, Aug. 2019.

[34] T. K. Roy, M. A. Mahmud, S. N. Islam, N. Rajasekar, K. M. Muttaqi, and A. M. T. Oo, "Robust adaptive direct power control of grid-connected photovoltaic systems," in *Proc. IEEE Int. Conf. Power Electron., Smart Grid Renew. Energy*, Jan. 2020, pp. 1–6.

[35] T. K. Roy, M. A. Mahmud, A. M. T. Oo, and M. E. Haque, "Robust nonlinear adaptive backstepping controller design for three-phase grid-connected solar photovoltaic systems with unknown parameters," in *Proc. IEEE Power and Energy Society Gen. Meeting*, Nov. 2016, pp. 1–5.

[36] Y. Li, S. Tong, and T. Li, "Direct adaptive fuzzy backstepping control of uncertain nonlinear systems in the presence of input saturation," *Neural Comput. Appl.*, vol. 23, no. 5, pp. 1207–1216, 2013.

[37] J. Dong, Q. Hou, and M. Ren, "Control synthesis for discrete-time T-S fuzzy systems based on membership function-dependent H_∞ performance," *IEEE Trans. Fuzzy Syst.*, vol. 28, no. 12, pp. 3360–3366, Dec. 2020.
[38] S. C. Tong, Y. M. Li, G. Feng, and T. S. Li, "Observer-based adaptive fuzzy backstepping dynamic surface control for a class of MIMO nonlinear systems," *IEEE Trans. Syst., Man, Cybern. B, Cybern.*, vol. 41, no. 4, pp. 1124–1135, Aug. 2011.
[39] Q. Hou and J. Dong, "Adaptive fuzzy reliable control for switched uncertain nonlinear systems based on closed-loop reference model," *Fuzzy Sets Syst.*, vol. 385, pp. 39–59, Apr. 2020.
[40] A. Govindharaj and A. Mariappan, "Adaptive neuralback stepping controller for MPPT in photo voltaic systems," in *Proc. IEEE Int. Conf. Intell. Techn. Control, Optim. Signal Process. (INCOS)*, Apr. 2019, pp. 1–6.
[41] F.-J. Lin, S.-G. Chen, and I.-F. Sun, "Adaptive backstepping control of six-phase PMSM using functional link radial basis function network uncertainty observer," *Asian J. Control*, vol. 19, no. 6, pp. 2255–2269, Nov. 2017.
[42] S. Khorashadizadeh and M. M. Fateh, "Robust task-space control of robot manipulators using legendre polynomials for uncertainty estimation," *Nonlinear Dyn.*, vol. 79, no. 2, pp. 1151–1161, Jan. 2015.
[43] J. C. Mason, H. David, and C. Chebyshev, *Polynomials*. New York, NY, USA: Chapman & Hall, 2002.

ARUNPRASAD GOVINDHARAJ (Student Member, IEEE) received the B.E. degree in electrical and electronics engineering from the Hindustan College of Engineering, Chennai, India, in 2007, and the M.E. degree in applied electronics from the College of Engineering, Anna University, Chennai, in 2010. He is currently pursuing the Ph.D. degree in electrical engineering with Annamalai University, Chidambaram, India. He is currently working as an Assistant Professor with the Electrical and Electronics Engineering Department, Galgotias College of Engineering and Technology, Greater Noida, Uttar Pradesh. His current research interest includes adaptive nonlinear controllers for power electronic converters for the DC and AC microgrid.

ANITHA MARIAPPAN received the degree in electrical and electronics and the master's degree (Hons.) in power systems from Madurai Kamaraj University, India, in 1991 and 1994, respectively, and the Ph.D. degree from Annamalai University, Tamil Nadu, India, in 2009. She has been working as a Teaching Faculty with Annamalai University, since 1997. She is currently working as a Professor with the Electrical Engineering Department, Annamalai University. She is a fellow of the Institution of Engineers. Her current research interests include the areas of power system restructuring, optimization problems, power system reliability problems, meta-material-based antennas, routing protocols for mobile *ad-hoc* networks, and adaptive controllers for power electronic circuits. She has around 50 articles in her credit in national and international level.

A. AMBIKAPATHY (Member, IEEE) received the Ph.D. degree. She is having 18 years of teaching experience. She is currently working as the Head of the Department of Electrical and Electronics Engineering and the Head of the IPR Cell at the Galgotias College of Engineering College and Technology. She has authored nine national and one international engineering books. She has filed nine Indian and five international patents, and published more than 40 research papers in various reputed international journals (SCOPUS and SCI) and conferences. She is involved in various funded projects from government organizations, such as MSME and Dr. Abdul Kalam Technical University, Lucknow. She has received various awards, including the Women Research Award International from Organization of Scientific Research and Development, the International Award for Women Leadership from World Federation Science and Technology and Research foundation of India, and the Dedicated Services Award from Rotary Club of Delhi South End. She is a reviewer of many reputed international journals. She also delivers expert lecture on various topics, such as awareness on IPR, motivational way to inspire students, and implementation of solar micro-plant at distribution side. During her service as the head of department, she made MOU with different industries and through which has organized many events.

VIKAS SINGH BHADORIA (Member, IEEE) received the B.E. and M.E. degrees in electrical and electronics engineering from RGPV, Bhopal, India, in 2005 and 2009, respectively, and the Ph.D. degree in power system from Gautam Buddha University, Greater Noida, Uttar Pradesh, India, in 2018. He is currently working as an Associate Professor with ABES Engineering College, Ghaziabad. His research interests include power system planning, power system reliability, and power system restructuring.

HASSAN HAES ALHELOU (Senior Member, IEEE) is currently a Faculty Member with Tishreen University, Latakia, Syria. He is also with the University College Dublin, Dublin, Ireland. He has published more than 130 research papers in the high-quality peer-reviewed journals and international conferences. He has participated in more than 15 industrial projects. His research interests include power systems, power system dynamics, power system operation and control, dynamic state estimation, frequency control, smart grids, microgrids, demand response, load shedding, and power system protection. He is included in the 2018 Publons list of the top 1% best reviewer and researchers in the field of engineering. He was a recipient of the Outstanding Reviewer Award for *Energy Conversion and Management* journal, in 2016; *ISA Transactions* journal, in 2018; *Applied Energy* journal, in 2019; and many other awards. He was also a recipient of the Best Young Researcher in the Arab Student Forum Creative among 61 researchers from 16 countries at Alexandria University, Egypt, in 2011. He has also performed more than 160 reviews for high-prestigious journals, including the IEEE TRANSACTIONS ON INDUSTRIAL INFORMATICS, the IEEE TRANSACTIONS ON POWER SYSTEMS, the IEEE TRANSACTIONS ON INDUSTRIAL ELECTRONICS, *Energy Conversion and Management*, *Applied Energy*, and the *International Journal of Electrical Power and Energy Systems*.